Journal of Materials Science and Engineering A 5 (3-4) (2015) 148-153
doi: 10.17265/2161-6213/2015.3-4.006

Titanium Oxide Nanoreservoirs Doped With Bee Venom Lyophilized Powder by Sol-Gel

J. Albino. Moreno R.[1*], Genaro Carmona G.[2], Efraín Rubio R.[3], Lilián-A. Moreno R.[3] and Fernando Moreno R.[4]

1. School of Chemical Sciences

2. Center of entailment and Energy Transfer

3. Institute of Physics, University City, San Manuel Colony, Puebla C. P. 72570, Puebla

4. Benemérita Universidad de Puebla

Abstract: Empirically, bee venom lyophilized powder has been applied in the treatment of various diseases such as: traumatic inflammations, rheumatism, osteoarthritis, rheumatoid arthritis, lumbar neuralgia, multiple sclerosis, radiculitis, arteriosclerosis of the extremities, lupus and peripheral nervous system disorders, treatment of high blood pressure, trophic ulcers, immune deficiencies, edema, asthma syndrome migraine, cardiovascular disorders, they are characterized by low efficiency of the myocardium, as cerebral vascular disorders and viral diseases such as herpes zoster and genital herpes. We synthesize titanium oxide nanoreservoir without impurities (TiO_2) and impregnated nanoreservoirs with 1.5 mg of bee venom lyophilized powder "in situ" (L-BV/TiO_2-15) by sol-gel. They were characterized by UV-VIS, FTIR and XRD. The anatase crystalline phase is evident for all TiO_2 nanoreservoir, they have a value of band gap energy of 3.0 eV. The average particle size of nanoreservois decreases with the incorporation of bee venom lyophilized powder (BV-L) in the mesh of TiO_2. The TiO_2 nanoreservoir has a value of 40.0 nm and the BV-L/TiO_2-15 nanoreservoir has a value of 30.0 nm. The bee venom lyophilized powder has a laminar texture.

Key words: TiO_2, bee venom lyophilized powder, nanoreservoirs, sol-gel, XRD, FTIR, SEM.

1. Introduction

Beevenom Lyophilized powder (BV-L), is one of the most important natural beekeeping products in the treatment of various diseases. It has been demonstrated empirically in the treatment of musculoskeletal and cancer cells. The lyophilized bee venom is a rich source of pharmacologically active peptides [1, 2]. In ancient civilizations it was used for medicinal purposes[3]. In oriental medicine has been used as a treatment for inflammatory diseases as in the case of rheumatoid arthritis and confers pharmacological properties and therapeutic actions [4, 5]. The major component of bee venom lyophilized powder is melittin, peptide with great contributions in the treatment of cancer, leukemia, sciatic neuralgia, osteosarcoma, melanoma and mammary gland cancer [6-8]. Melittin exerts a greater therapeutic action, representing up to 50% dry weight of venom. Its physiological action is raising the level of blood cortisol and is not accompanied by undesirable side effects, such as, usually with steroids commonly used to treat these types of conditions. In cases where treatment requires the use of radiation therapy, the bee venom lyophilized powder has radio protective effects, which has been shown in research conducted using mice as an experimental model, reporting a 64%, compared to animals that were not inoculated with bee venom lyophilized powder [9].

Corresponding author: J. Albino. Moreno R., doctor, research fields: development of nanomaterials, nanocatalysts, nanosoportes and nanoreservorios. E-mai: albinomx@yahoo.com.

2. Experiments

The titanium oxide (TiO_2) and titanium oxide were doped with bee venom lyophilized (BV-L/TiO_2-15) nanoreservoirs they obtained from a homogeneous solution of 150.0 mL of isopropyl alcohol (Sigma-Aldrich 99.7%) and 6.0 mL of deionized water

in a reflux system to 70 °C and with constant stirring.

2.1 Synthesis of TiO_2 nanoreservoirs

Added the homogeneous solution prepared previously in a three necked reactor. The temperature is increased 70 °C and added dropwise 21.0 mL of titanium IV isopropoxide (Sigma-Aldrich 97.0%). Subsequently, the gel is immersed in a plastic vessel with containing ice water for 20 min at 2 °C. The TiO_2 aerogel are obtained by extracting the solvent in a rotary evaporator with the help of a vacuum pump.

2.2 Synthesis of L-BV/TiO_2-15 nanoreservoirs

0.0015 g bee venomlyophilized powder is also added to the previously prepared homogeneous solution. The same process is performed for the synthesis of BV-L/TiO_2-15 nanoreservoirs, mentioned in the part of the synthesis of nanoreservoirs TiO_2.

3. Techniques of Characterization

The TiO_2 and BV-L/TiO_2-15 nanoreservoirs and bee venom lyophilized powder (BV-L), are characterized by Infrared spectroscopy, with a spectrophotometer of Fourier transform Digilab SCIMITAR Series; Ultraviolet-visible spectroscopy with a UV-VIS spectrophotometer, Varian Cary Model 100 was used, with integrating sphere reflectance diffuse. The study of diffraction of x-rays was made with a spectrophotometer X-Ray Diffraction (XRD)-Discover D8, Lynx Eye Bruker reader, voltage of 40 Kv. The micrographs were made with a scanning electron microscope, JEOL JSM-6610LV. Elemental analysis was made with a team of Energy Spectroscopy Scattered.

4. Results and Discussion

4.1 Ultraviolet-Visible Spectroscopy (UV-VIS).

The UV-VIS spectrum of bee venom lyophilized powder (BV-L) is shown in Fig. 1. The BV-L presents two absorption peaks which are representative. The absorption peak at 270.8 nm (ultraviolet region) and the absorption peak to 537.8 nm (visible region). The absorption band at 270.8 nm corresponds to the excitation mode of the amino groups (secondary amine, NH); associated to the peptide chain and the absorption band located at 537.8 nm, corresponding to the excitation mode of the benzene group shifted to higher energy regions of the amino groups and aldehydes, associated to the amino acid.

The Table 1 presents some optical properties of bee venom lyophilized powder. The absorption band at 270.8 nm, it absorbed in the far-ultraviolet region spectrum with a frequency of 1.1×10^{15} Hz. And the absorption band at 537.8 nm it absorbed in the visible region spectrum (green color) with a frequency of 5.6×10^{14} Hz.

There is no variation in the optical and electronic parameters when to TiO_2 material is doped with 0.0015 g of VA-L powder. The absorption band for both TiO_2 and BV-L/TiO_2-50 nanomaterials is very much similar, they presented in 407.3 nm (for TiO_2) and 418.2 nm (for BV-L/TiO_2-15). This variation is due to the presence of the BV-L powder into the mesh of TiO_2 nanomaterial. The value of 2.96 eV is assigned to the anatase crystalline phase, corresponding to wavelength

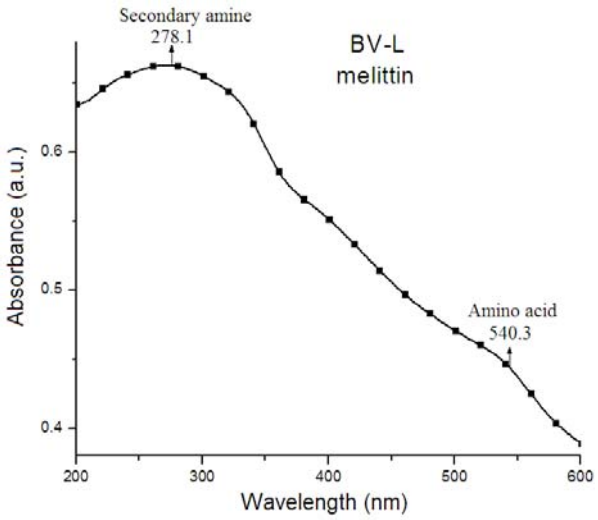

Fig. 1 UV-VIS spectrum of L-BV powder.

Table 1 Optical properties of bee venom lyophilized powder.

Material	λ (nm)	E (eV)	υ (Hz)	spectral region
BV-L	270.8	4.5	1.1×10^{15}	Far-UV
	537.8	2.3	5.58×10^{14}	VIS (green color)

of 418.2 nm [10], this value is very much similar to 3.04 eV of BV-L/TiO_2-15 nanomaterials. Thus, the concentration of BV-L powder not changes the anatase phase of TiO_2 nanomaterial (Table 2).

In Fig. 2, the UV-VIS spectra of TiO_2 and BV-L/TiO_2-15 nanomaterials are shown, respect to BV-L powder.

4.2 InfraredSpectroscopy (IR)

The IR spectra of BV-L powder, TiO_2 and VBV-L/TiO_2-15 nanomaterials are shown in Fig. 3.

According to what was reported, the BV-L powder, bee venom lyophilized powder contains chemical compounds as: melittin (50 wt%), peptides (2 wt%) as apamin, enzymes such as lecithinase A (3 wt%), hyaluronidase, fosfalipasa A (12 wt%) as riboflavin, formic acid, hydrochloric acid, orthophosphoric acid, histamine, choline, tryptophan and sulfur. IR spectrum of the BV-L powder shows an absorption band at 3261.6 cm^{-1}, assigned to the stretching vibrational mode of asymmetrical methyl group ($\nu_{C\text{-}H}$). The absorption band at 2,956.8 cm^{-1}, assigned to the stretching vibrational mode of asymmetrical methylene group (ν_{CH2}) assignation to alcohol and aldehyde groups. The absorption band located at 1,567.6 cm^{-1} is assigned to deformation vibration mode of the secondary amino group ($\nu_{N\text{-}H}$). The absorption band located at 1,098.9 cm^{-1}, assigned to the bending vibrational mode of ether group ($\nu_{C\text{-}O\text{-}C}$). The absorption band located at 632.6 cm^{-1}, assigned to the strain vibrational mode of the Benzene-H species outside the plane of the ring ($\delta_{\varnothing\text{-}H}$) and to the strain vibrational mode of the secondary amino group ($\delta_{N\text{-}H}$).

The TiO_2 (black curve) shows an absorption bandlocated at 3,220.0 cm^{-1}, is assigned to the stretching vibrational mode of the OH species ($\nu_{O\text{-}H}$). It correspond to the hydroxylgroups (OH^-), water (H-OH), solvent (1-butanol, R-OH) and the hydroxylation of gel (Ti-OH). These functional groups are present in the pores of TiO_2; they formed during the first stage of gelation [11]. The absorption band located

Table 2 Optical and electronic properties of TiO_2 y VA/TiO_2-15 nanomaterials.

Nanomaterial	λ (nm)	E_g (eV)	υ (Hz); ($x10^{14}$)	SpectralRegion
TiO_2	418.2	2.96	7.1	UV-VIS (violeta)
BV-L/TiO_2-15	407.3	3.04	7.4	UV-VIS (violeta)

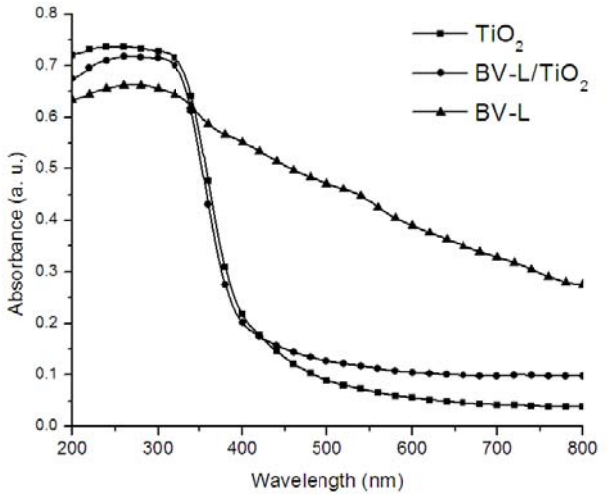

Fig. 2 UV-VIS spectrum of TiO_2 and BV-L/TiO_2-15 nanomaterials, respect to BV-L powder.

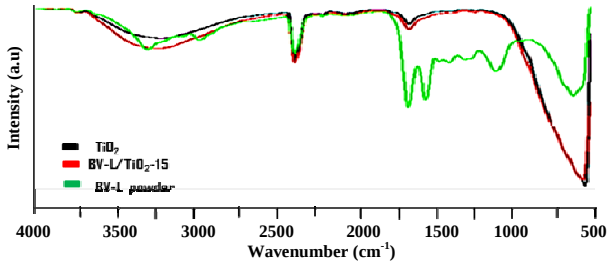

Fig. 3 FTIR spectrum of TiO_2 and BV-L/TiO_2-15 nanomaterials, respect to BV-L powder.

at 3,692.0 cm^{-1}, is assigned to terminal vibration mode of the OH^-groups ($\nu_{O\text{-}H}$) [12, 13]. The absorption band located at 1,635.0 cm^{-1}, is assigned to bending vibration mode of the hydroxyl groups of water that is present on the surface of TiO_2 nanomaterial($\nu_{O\text{-}H}$), as so to deformation vibration mode of the OH^- groups ($\delta_{O\text{-}H}$) [14]. The absorption band located at 1,365.0 cm^{-1}, 1 is assigned to oxidation vibration mode of the TiO_2 nanomaterial, due to impurities present during the condensation process of the material and the ethoxy groups ($\nu_{C\text{-}O}$) who have not reached react (Ti-OEt). The stretching absorption band located at 1,210.0 cm^{-1}, is assigned to C-C and C-O species of the bridge methoxy groups [15, 16]. In the spectral region of low energy

absorption band located at 530.0 cm^{-1}, is assigned to bending vibration mode of the Ti-O species (ν_{Ti-O}) [16, 17].

The IR spectra of BV-L/TiO_2-15 nanomaterials are very similar to IR spectra of TiO_2 nanomaterials, this may be due to the low concentration by weight of the BV-L powder on the TiO_2 nanomaterial.

4.3 X-ray Diffraction.

In analyzing the atomic scattering factors, a pair of neutral atoms were used [18]. The BV-L/TiO_2-15 and TiO_2 nanoreservoirs present the anatase phase, according to values of the intensity peaks with a diffraction angle of 2Θ = 25.5° (101 reflection), 38.2°, 47.9° and 54.7°, corresponding to the reflection planes (101), (004), (200) and (21), respectively, as shown on Fig. 4.

The X-ray diffraction of the BV-L powder is shown in the Fig. 5. It is crystalline. The X-ray diffraction of the BV-L powder is also shown in the figure 5. It presents five intensity peaks with a diffraction angle of 2Θ = 9.29°, 12.9°, 18.8°, 29.8° and 42.1°.

4.4 Scanning Electron Microscopy (SEM).

The micrograph of TiO_2 nanomaterial is presented in Fig. 5. The TiO_2 nanomaterial showed crystal morphology of agglomerated particles as semispherical, with an average particle size of 40.0 nm.

The micrograph of BV-L/TiO_2-15 nanomaterial is shown in Fig. 6. The BV-L/TiO_2-15 nanomaterial showed crystal morphology of agglomerated particles semispherical, with an average particle size of 30.0 nm.

The texture of BV-L powder showed a sheet form (plates). These plates have small cylinders form with a length between 1 nm to 2 nm and a diameter of approximately 3.0 nm to 5.0 nm. The plates have a length of about 30.0 nm to 60.0 nm. Certain of these crystalline structures are observed with hexagonal and cylindrical geometric orientations.

4.5 Energy Dispersed Spectroscopy (EDS)

The results experimental of EDS of TiO_2 nanoreservoir

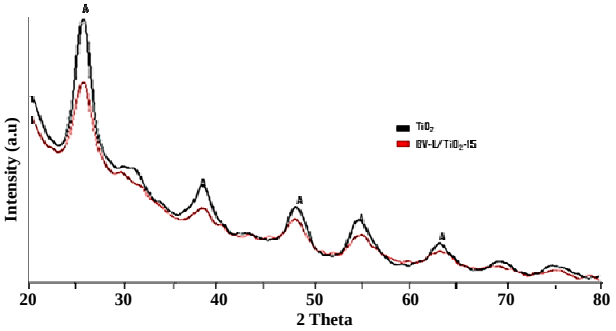

Fig. 4 X-ray diffraction of the TiO_2 and BV-L/TiO_2-15 nanoreservoirs.

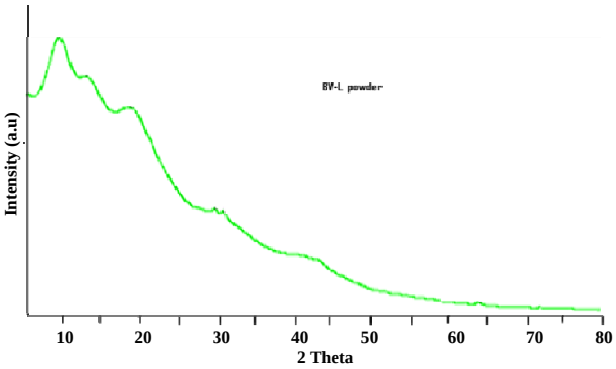

Fig. 4 X-ray diffraction of BV-L powder.

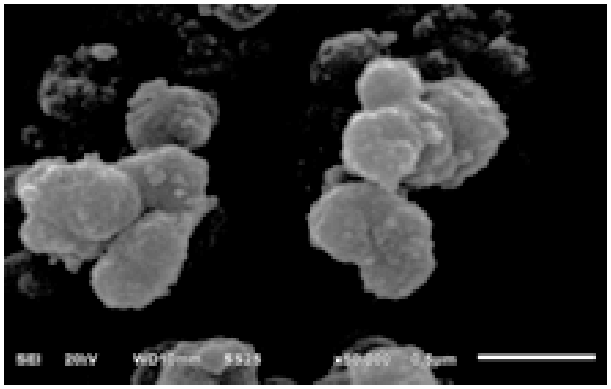

Fig. 5 SEM micrographs of TiO_2 nanomaterial to 50,000 ×.

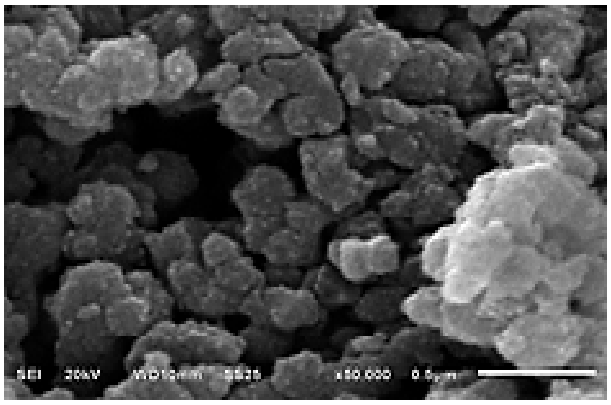

Fig. 6 SEM micrographs of BV-L/TiO_2-15 nanomaterial to 50,000 ×.

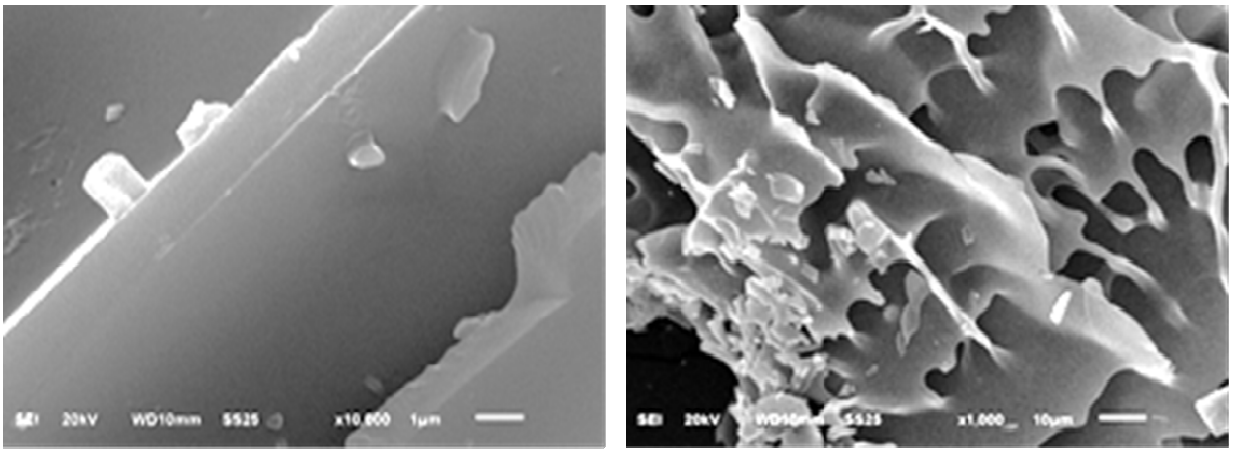

Fig. 7 SEM micrographs of BV-L powder to 10,000 × and 1,000 ×.

Table 3 EDS of TiO_2 nanomaterial.

Elements	Mass (%)	Atoms (%)
Carbon (C)	5.74	11.41
Titanium (Ti)	52.39	62.47
Oxygen (O)	41.87	26.11
Total	100.00	

Table 4 EDS of BV-L powder.

Elements	Mass (%)	Atoms (%)
Carbpn (C)	65.28	72.41
Oxygen (O)	31.86	26.53
Sulfur (S)	0.86	0.36
Chlorine (Cl)	0.73	0.28
Potassium (K)	0.77	0.26
Calcium (Ca)	0.50	0.17
Total 100		

Table 5 EDS of BV-L/TiO_2-15 nanomaterial.

Elements	Mass (%)	Atoms (%)
Carbon (C)	16.58	17.28
Oxygen (O)	37.92	31.58
Titanium (Ti)	45.28	50.98
Sulfur (S)	0.09	0.04
Chlorine (Cl)	0.07	0.03
Potassium (K)	0.02	0.01
Calcium (Ca)	0.04	0.08
Total 100		

have shown a 52.38 wt% of titanium and 41.87 wt% of oxygen as shown the Table 4. Those results indicate that the minimum formula is $TiO_{2.4}$ regarding to the molecular formula of TiO_2, indicating that for each atom of titanium, there is approximately 2, 4 oxygen atoms.

The results experimental of EDS of BV-L-15 powder indicates the presence of the elements as sulfur (S), chlorine (Cl), potassium (K) and calcium (Ca), they are identified in the chemical formula of BV-L-15 powder, as shown the Table 4. The presence of sulfur is a key element, it part of the structure of degranulador peptide of mast cell inflammatory component of bee venom. The presence of Cl and K atoms are reported by N.P. Ioirich [19], as part of the active ingredients of BV-L powder and the carbon atoms are present in enzymes and peptides (as C-C, C = O, C-O, C-N and C-H), essential components in the venom of lyophilized bee.

Regarding to the VA-L/TiO_2-15 nanoreservoirs, the presence of elements such as sulfur, chlorine, potassium and calcium, as shown in the Table 6, it confirms the existence of the BV-L powder in mesh of TiO_2 nanomaterial.

5. Conclusions

Bee venom is present in the mesh of TiO_2 as shown by the study of EDS. The presence of anatase in the TiO_2 and VA-L/TiO_2-15 is observed. The small concentration of BV-L (0.0015 g) does not modify the crystalline phase of TiO_2; however, reduces the average particle size of the TiO_2 nanomaterial of 40.0 nm (for TiO_2) to 30.0 nm (for BV-L/TiO_2-15). The corresponding functional groups of lyophilized bee venom are mainly those of melittin, peptide (opamin),

choline, and phospholipase and rivoflamin.

References

[1] González, A., and Bernal, R. 1998. *Bee Venom (News and Perspectives)*. Pablo de la Torriente press.

[2] Trevor, S., and Darlington, G. 2001. *As drugs act the Pills, Potions and Poisons*, edited by Arial. Autonomous University of Barcelona.

[3] Urtubey, N. 2003. *Apitoxin (Bee Venom to the Apitoxin for Medical Use)*. 2th Edition. Argentina: Santiago del Estero.

[4] Jae-Dong, L. 2004. "Anti-Inflammatory Effect of Bee Venom on Type II Collagen Induced Arthritis." *The American Journal of Chinese Medicine* 32 (3): 361-7.

[5] Choong-Hee, W., Seong-Sun, H., and Christopher, M-H. K. 2000. "Efficacy of Apitox (Bee Venom) for Osteoarthritis: a Randomized Active-Controlled Trial." *The Journal of American Apitherapy Society* 7: 3.

[6] Ćurić, S., Tadić, Z., Valpotić, I., Sulimanović, D., and Baŝić, I. 1992. "The Effect of Bee Venom on Tumor Growth and Metastasis Formation of Mammary Carcinoma in CBA Mice." *Veterinarsky" University of Zagreb* 62: 31-5.

[7] Peña, L., Pineda, M. E., and Hernández, M. 2006. "Natural Toxins: Bees and Poisons." *AVFT.* 25 (1): 6-10.

[8] Goldsby, R., Kindt, T., Osborne, B., and Kuby, J. 2006. *Immunology*, 5th edition., Mc Graw Hill Interamerican.

[9] Asís, M. 2007. "Apitherapy" 101 for all. 3th edition. Miami, Florida.

[10] Martínez, A., Acosta, D., and López, A. 2003. "Effect of Sn Content on the Physical Properties of Thin Films of TiO_2." *Superficies y Vacío.* 16 (1): 5-9.

[11] Ouyang, A., Nakayama, A., Tabada, K., and Suzuki, E. 2012. *J. Phys, Chem, B* 104.

[12] Hadjiivanov, K., Avreyska, V., Klissurski, D., and Marinova, T. 2002. *Langmuir* 18: 1619.

[13] Bensitel, M., Lamotte, V., Saur, O., and Lavalley, J. 1987. *Spectrochim. Minute* 43A: 1487.

[14] Jacob, K., Knözinger, E., and Benies, S. J. 1993. *Mater. Chem.* 3: 65.

[15] Indovina, V., Occhiuzzi, M., Pietrogiacomi, D., and Tuti, S. 1999.

[16] Ouyang, F., Kondo, J., Maruya, K., and Domen, K. 1997. *J. of Phys. Chem. B* 101: 4867.

[17] Zaki, M., Hasan, M., and Pasupulety, L. 2001. *Langmuir* 17: 768.

[18] International Centre for Diffraction Data (1997), PCPDFWIN v. 1.30.

[19] Iorich, N. 1981. *As Abelhas Farmacêuticas Com Asas*. 2edicão. A Ciência ao alcance de todos. Editora Mir Moscovo. U.R.S.S.